Environmental Science Nano

PAPER

View Article Online
View Journal | View Issue

Cite this: *Environ. Sci.: Nano*, 2019, **6**, 136

Photolysis of graphene oxide in the presence of nitrate: implications for graphene oxide integrity in water and wastewater treatment†

Lin Duan,[a] Tong Zhang,[a] Weihua Song,[b] Chuanjia Jiang,[a] Yan Hou,[a] Weilu Zhao,[a] Wei Chen *[a] and Pedro J. J. Alvarez[c]

Received 13th June 2018,
Accepted 2nd November 2018

DOI: 10.1039/c8en00637g

rsc.li/es-nano

Despite the widespread use of graphene oxide (GO) in diverse applications and increasing interest in its inclusion in some water treatment devices, mechanistic understanding of photochemical GO transformations is limited. This is an important knowledge gap relevant to GO performance and durability. We examined the reaction pathways and products of a GO suspension under UV irradiation in the presence of nitrate, a common anion in water and wastewater treatment processes. As the nitrate concentration increased, the dominant pathway of GO transformation changed from direct photolysis to indirect photolysis enhanced by the production of hydroxyl radicals (•OH) during UV irradiation of nitrate. At environmentally relevant concentrations (*e.g.*, 1 mM), nitrate induced significant fragmentation of the GO nanostructure. The significant effects of •OH on GO morphology and surface properties were verified by negative-control tests, including deoxygenation of the suspension, reactive oxygen species (ROS) inhibition and radical trapping, and by γ-radiolysis, known to generate a single ROS: •OH. Supplemental photolysis experiments conducted using graphite demonstrated that the main reaction pathways of the indirect photolysis of GO not only include the oxidation reactions between •OH and the oxidized domains of GO, but also the electrophilic addition reaction between •OH and the aromatic domains. These findings have significant implications for GO integrity and durability in systems involving incidental or purposeful exposure to UV irradiation.

Environmental significance

Graphene oxide (GO) materials are a promising class of carbonaceous nanomaterials that hold great promise for enhancing water and wastewater treatment (*e.g.*, membranes and adsorbents). When used in treatment processes, GO materials may be exposed to various chemical and biological agents, resulting in alterations of their morphologies and surface properties. This may affect not only the performances of GO-based materials, but also their integrity and durability. This study shows that the presence of nitrate, one of the most common inorganic anions in water and wastewater, at environmentally relevant concentrations significantly enhances the photolysis of GO materials, resulting in disintegration of GO nanosheets, as well as substantial alterations of GO surface functional groups. These results underscore the need to understand the photochemical transformation mechanisms of carbonaceous nanomaterials and the associated implications for their performance and durability.

1 Introduction

Graphene oxide (GO) is one of the promising carbonaceous nanomaterials of significant interest for a number of applications, such as polymer composite fabrication, electronic devices, energy storage, and biomedicine.[1–3] Owing to its high surface area and abundant surface O-functional groups, GO has also been considered to improve water and wastewater treatment devices such as adsorbents, catalysts, and filtration membranes.[4–9] Moreover, a variety of metal/metal oxide nanoparticles and polymers can be anchored to GO to achieve higher efficiency for contaminant removal.[10] During applications in water or wastewater treatment, GO will likely be exposed to various chemical and biological agents, which may result in the transformation of GO[11–13] and compromise the performance, integrity, and durability of these materials. Transformation of GO may also result in the formation of toxic contaminants, such as oxygenated polycyclic aromatic hydrocarbon species.[14,15]

[a] *College of Environmental Science and Engineering, Ministry of Education Key Laboratory of Pollution Processes and Environmental Criteria, Tianjin Key Laboratory of Environmental Remediation and Pollution Control, Nankai University, 38 Tongyan Road, Tianjin 300350, China.*
E-mail: chenwei@nankai.edu.cn; Fax: +86 22 85358169; Tel: +86 22 85358169
[b] *Department of Environmental Science & Engineering, Fudan University, 220 Handan Road, Shanghai 200433, China*
[c] *Department of Civil and Environmental Engineering, Rice University, 6100 Main Street, Houston, Texas 77005, USA*

† Electronic supplementary information (ESI) available. See DOI: 10.1039/c8en00637g

Ultraviolet (UV) irradiation, a commonly adopted approach for disinfection and contaminant degradation,[16] has been shown to induce photochemical transformation of GO.[15,17–25] Photolysis of GO under UV irradiation may occur through both direct and indirect pathways.[15,18–25] GO can undergo direct photolysis by acting similarly to photo-reactive semiconductors to generate electron–hole pairs, leading to the oxidation of O-functional groups to a higher oxidation state (quinones and carboxylic acids) by the holes or the reduction of O-functional groups by trapped-electrons, finally resulting in the loss of O-containing functional groups and the appearance of cavities and defects on GO nanosheets.[19–22,25] A limited number of studies have also been conducted to understand indirect photolysis of GO. It was reported that GO can undergo indirect photolysis in the presence of H_2O_2 or Fenton reagents ($Fe^{2+}/Fe^{3+}/H_2O_2$).[15,23,24] However, while external reactive oxygen species (ROS) was assumed to play an important role in indirect photolysis of GO, little is known about the photolysis products of GO by external ROS source reagents at environmentally relevant concentrations, and the relative contribution of direct *vs.* indirect photolysis in such systems. Moreover, the specific reactivity of different GO domains toward ROS is unclear. For instance, it has been proposed that indirect photolysis of GO by ROS is mainly due to the oxidation reactions between ROS and the oxidized domains, and the reaction rates depend strongly on the oxidation degree of GO.[15,23–26] Nonetheless, other researchers proposed that the pristine sp^2-carbon structures are the primary active sites to scavenge radicals, based on the observed antioxidant effects of GO.[27]

Natural water and wastewater often contains complex constituents (*e.g.*, natural organic matter and inorganic anions) that can induce the generation of ROS.[28–31] One of the important precursors for these ROS is nitrate, a common inorganic anion in water as a consequence of agricultural application of nitrogenous fertilizers and manures as well as the discharge of industrial nitrogenous wastes.[32,33] The maximum contaminant level (MCL) for nitrate is 10 mg L^{-1} nitrate-nitrogen in drinking water supply, but nitrate concentration can reach much higher levels, with concentrations up to hundreds of mg L^{-1} in groundwater of agriculture areas.[29,34] Many ROS, such as nitrogen oxide radicals ($^{\bullet}NO$ and $^{\bullet}NO_2$), superoxide radical anion ($O_2^{\bullet-}$) and hydroxyl radical ($^{\bullet}OH$), can be generated when nitrate is exposed to UV.[29,32,35,36] Thus, we postulate that when GO is exposed to UV irradiation in the presence of nitrate, the radicals generated may result in indirect photolysis of GO. To date, the potential effects of nitrate-induced indirect GO photolysis, at environmentally relevant nitrate concentrations, on GO physicochemical properties have not been investigated.

This study seeks to advance mechanistic understanding of GO photolysis and reaction pathways in the presence of nitrate. The effects of nitrate were examined by comparing changes in morphology, structure and surface O-functional groups of GO induced by UV treatment in the presence and absence of nitrate, using combined spectroscopic techniques. Different nitrate concentrations were tested in photolysis experiments to identify the relative contribution of indirect photolysis of GO in the presence of nitrate. Anaerobic experiments, ROS inhibition experiments and radical trapping were conducted as negative controls and γ-radiolysis experiments as a positive control to discern the predominant reactive species responsible for the observed nitrate effects. Moreover, functionality-free, pure graphite was used as a model material to identify the reactivity of the aromatic domains of GO during the indirect photolysis of GO.

2 Experimental

2.1 Materials

GO (>99%) was purchased from Nano Materials Tech Co. (Tianjin, China). According to the supplier, the product was synthesized from graphite using a modified Hummers method. Pure graphite (99.99%) was purchased from Sigma Aldrich (St. Louis, MO, USA). Sodium nitrate ($NaNO_3$), sodium sulfate (Na_2SO_4) and sodium chloride (NaCl) of chemical grade were obtained from Guangfu Tech Co. (Tianjin, China). Isopropylamine and parachlorobenzoic acid (*p*CBA) was purchased from Mackin biochemical Co. (Shanghai, China). Humic acid (HA) was purchased from Guangfu Tech Co. (Tianjin, China).

2.2 Photolysis experiments

An aqueous stock suspension of GO was prepared using the following procedures according to our previous study.[37] First, approximately 60 mg of GO powder was added to 300 mL of deionized (DI) water and mixed using a magnetic stir bar for 0.5 h, and then the mixture was sonicated (600 W, 40 MHz, SB25-12DTDN, Sicentzbio Tech Co. Ningbo, China) for 4 h in a water bath at 30 °C. Finally, the well-mixed GO suspension was kept in dark at 4 °C until use. The working GO suspension was prepared for each irradiation experiment by diluting the GO stock suspension with DI water to a concentration of 10 mg L^{-1}.

Photolysis experiments were carried out in 60 mL customized quartz tubes using a XPA-7 photoreactor (Xujiang, Nanjing, China) equipped with a 500 W medium pressure mercury (Hg) lamp in the center of the photoreactor. To initiate a photolysis experiment, 50 mL of 10 mg L^{-1} GO suspension was added in the quartz tube with or without sodium salts ($NaNO_3$, Na_2SO_4 and NaCl) and then sealed with a ground glass stopper and completely mixed using a magnetic stir bar in the dark for 1 h. The reactor was submerged in a thermostatic water bath (25 °C), and exposed to the 500 W medium pressure Hg lamp. The spectrum of UV light emitted from the Hg lamp was measured with a radiometer (RPS900-R, International Light, USA) and presented in the ESI† (Fig. S1). At determined time periods during irradiation, GO suspension in the quartz tube was removed from the reactor and sacrificed for analysis. To test the effects of nitrate, stock solution of different sodium salts ($NaNO_3$, Na_2SO_4 and NaCl) was added to the working GO suspension to reach a final

anion concentration of 1 mM. $NaNO_3$ was also added at concentrations of 0.05, 0.1 and 5 mM to identify the effects of nitrate concentration on GO photolysis. To examine the effects of variable water solution chemistry on GO transformation in the presence of nitrate, additional photolysis experiments were carried out by adding different concentrations (1, 5, 10, 50 or 100 mg L^{-1}) of humic acid (as representative natural organic matter), and by using tap water or pond water.

For experiments under anaerobic conditions, GO suspension (50 mL) was purged with high-purity N_2 or Ar gas for at least 1 h and sealed to achieve a dissolved O_2-deficient environment prior to UV irradiation.[38,39] To identify the ROS during UV irradiation in the presence of nitrate, 1% (v/v) isopropylamine and 0.5 ppm pCBA were used as a scavenger and a probe for $^{\bullet}OH$, respectively. All experiments conducted under UV-irradiation were performed in duplicate. Additionally, 10 mg L^{-1} GO aqueous suspension saturated with nitrous oxide (N_2O) was subjected to different doses of gamma (γ) radiation (400, 800, 1600 and 3000 Gy) to further identify the role of $^{\bullet}OH$ in GO photolysis,[24,25] using ^{137}Cs γ-rays (γ-Cell 40, Atomic Energy of Canada, Ontario, Canada) at a dose rate of 1.0 Gy min^{-1}.

2.3 Material characterization

The morphologies and structures of GO samples were characterized by transmission electron microscopy (TEM) (FEI Tecnai G2100 F-20, Hatfield, PA) and atomic force microscopy (AFM) (Veeco Multimode Nanoscope VIII, Santa Barbara, CA). The structural changes of GO after UV irradiation were monitored by UV-vis absorption (UV-2401 UV-vis spectrophotometer, Shimadzu, Japan), X-ray diffraction (XRD) (Rigaku D/max-2500, Japan) and Raman spectroscopy (Renishaw inVia Raman microscope, RM2000, UK). Surface chemistry properties of GO were characterized by X-ray photoelectron spectroscopy (XPS) (PHI 5000 VersaProbe, Japan). The photolysis products of GO were analyzed using electrospray ionization-mass spectrometry (ESI-MS, Xevo TQ-S, Waters, USA). Total organic carbon (TOC) concentrations were determined with a high sensitivity TOC analyzer (Shimadzu Scientific Instruments, Columbia, MD). Surface O-functional groups of the photo-transformed graphite were characterized by Fourier transform infrared (FTIR) transmission spectroscopy (110 Bruker TENSOR 27 apparatus, Germany).

3 Results and discussion

3.1 Photo-transformation of GO affected by nitrate

Changes of GO appearance and morphology. The physical appearance and morphology of GO varied remarkably depending on whether nitrate was present during UV irradiation (Fig. 1). For example, when a GO suspension (10 mg L^{-1}) was irradiated in the presence of 1 mM nitrate (the transformation product is referred to as GO-UV-nitrate), the color of the suspension became transparent in 2 h (Fig. 1c). However, in the system without nitrate, *i.e.*, irradiation of the GO suspension in DI water (the transformation product is referred to as GO-UV), the color of the suspension turned blackish in 2 h, and settlement of GO aggregates was evident (Fig. 1b). No distinguishable differences from GO-UV were observed when the GO suspension was UV-irradiated in the presence of sulfate or chloride (the reaction products are referred to as GO-UV-sulfate and GO-UV-chloride, respectively) (ESI† Fig. S2b and c), indicating a nitrate-specific effect on GO photolysis pathways. Moreover, no noticeable changes of the GO suspension were observed for the dark control sample (*i.e.*, GO suspension in nitrate receiving no UV irradiation; referred to as GO-dark) during the time course of the photolysis experiments (Fig. 1a). Photolysis experiments of GO with different nitrate concentrations showed that the nearly transparent color of GO suspension was only observed at nitrate concentrations of 1 mM and above, whereas for the two GO samples involving lower nitrate concentrations of 0.05 and 0.1 mM, no distinguishable differences from GO-UV were observed (ESI† Fig. S3). Apparently, the effects of nitrate were concentration-dependent. The significant effects of nitrate on GO

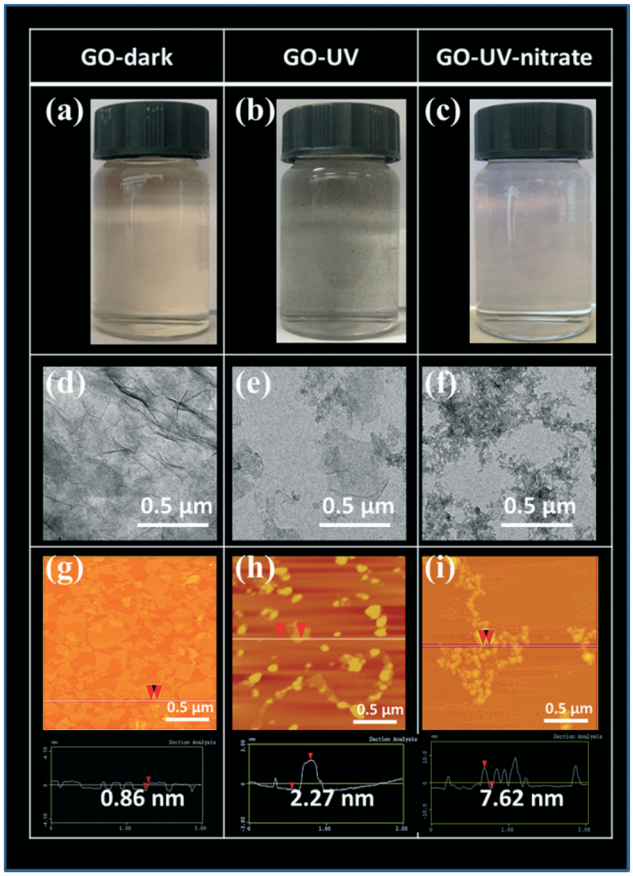

Fig. 1 Changes in GO suspension (10 mg L^{-1}) appearance and GO morphology after 9 h of UV irradiation, showing that the presence of nitrate (1 mM) significantly affected GO photo-transformation, as indicated by the color change of GO suspensions (a–c: photographs), morphology (d–f: TEM images) and size (g–i: AFM images) of GO samples. GO-dark, GO-UV, and GO-UV-nitrate represent GO suspension receiving no UV irradiation, GO suspension UV-irradiated in DI water, and GO suspension UV-irradiated in the presence of nitrate, respectively.

transformation were also observed in the presence of humic acid (up to 100 mg L^{-1}), as well as in tap water and surface water (ESI† Fig. S4).

TEM images showed significant damages of GO nanosheets for GO-UV-nitrate, wherein the smooth basal plane of GO nanosheets was disintegrated into small fragments (Fig. 1f). In contrast, GO-UV, GO-UV-sulfide and GO-UV-chloride showed larger pieces with irregularly shaped GO nanoflakes (Fig. 1e and ESI† Fig. S2e and f). The AFM images corroborated the significant effects of nitrate on GO photolysis (Fig. 1g–i, and ESI† Fig. S2g–i and S5). For GO-dark, the lateral sizes of GO nanosheets showed a broad distribution and the thickness of the nanosheets was mostly below 1 nm (Fig. 1g and ESI† Fig. S5); for GO-UV, GO nanoflakes with dominant square root of areas of 50–100 nm and thickness of 5–10 nm (Fig. 1h and ESI† Fig. S5) were observed, likely attributable to the aggregation of the photoreaction products. In comparison, GO-UV-nitrate consisted of numerous small-sized fragments with dominant square root of areas below 50 nm and thickness of 5–15 nm (Fig. 1i and ESI† Fig. S5), indicating the significant disintegration of GO flakes and increased tendency of aggregation.

Changes of GO structures. UV irradiation of GO suspension in the presence of nitrate also had significant influences on the structures of GO nanosheets, as evidenced by the changes of the UV-vis absorbance of GO suspension (Fig. 2). Specifically, the maximum absorption peak position (λ_{max}) exhibited red shifts for GO-UV, GO-UV-sulfide and GO-UV-chloride (Fig. 2a and ESI† Fig. S6), indicating the partial restoration of the π-conjugated structure.[24,40] In contrast, λ_{max} exhibited significant blue shifts for GO-UV-nitrate (Fig. 2b), indicating the damage of local π-conjugated structures.[24] Similar effects of nitrate on GO structural changes were observed in the presence of humic acid (ESI† Fig. S7). Moreover, UV-vis absorbance of GO suspension in the presence of different concentrations of nitrate further showed that the shift of λ_{max} seemed to be related to the amount of nitrate used (Fig. 3). At low nitrate concentration (0.05 or 0.1 mM), red shift of λ_{max} in UV-vis spectra of GO suspension was observed.[24,40] In contrast, with higher concentrations of nitrate (1 and 5 mM), blue shift of λ_{max} in the UV-vis spectra of GO suspension was observed.[24] This distinct concentration-dependent effect of nitrate on GO structure also suggested that the dominant reaction pathway of GO photolysis changed from direct photolysis to indirect photolysis with increasing nitrate concentration. Note that the threshold nitrate concentration that activated the secondary photolysis pathway in this study is only slightly higher than the MCL value of nitrate, indicating potential significant effects of nitrate in GO transformation in water and wastewater treatment.

The structural changes of GO from photolysis were further characterized by Raman and XRD analyses (ESI† Fig. S8). Even though UV irradiation both in the absence and presence of nitrate resulted in the reduction of GO as evidenced by the XRD patterns of GO-UV and GO-UV-nitrate, the Raman spectra showed that GO-UV-nitrate had a larger I_D/I_G (the ratio of the intensities of the D and G bands) value than did GO-UV, indicating a more significant decrease in the average size of the π-conjugated structures of GO nanosheets and an increase in the abundance of GO edges or defects when GO was UV-irradiated in the presence of nitrate.[1,15,20]

A series of low molecular-weight species as the photolysis products were detected in the mass spectrometry (MS)

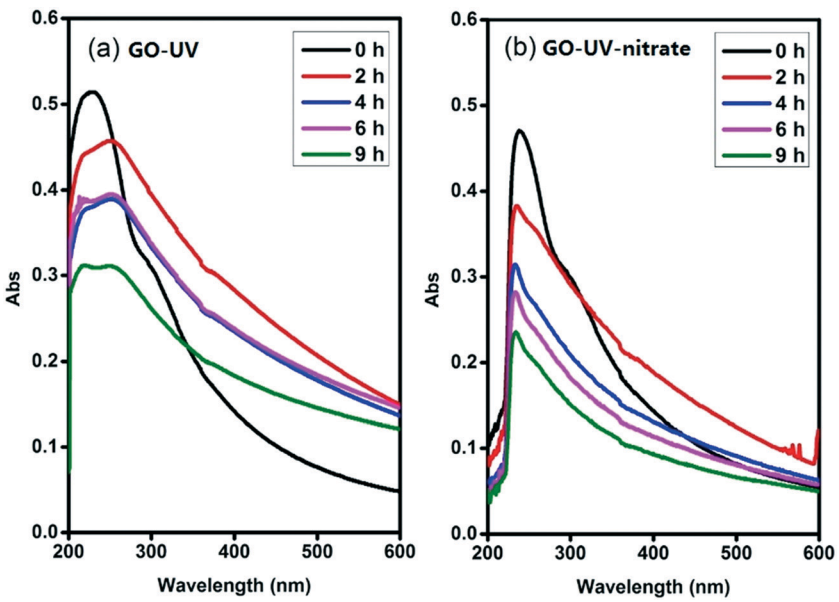

Fig. 2 UV-vis spectra of 10 mg L^{-1} GO suspensions before and after UV irradiation in the absence (a) or presence (b) of 1 mM nitrate, showing the significant effects of nitrate on GO photolysis. Structural changes of GO nanosheets are indicated by the shift of the maximum absorption peak position (λ_{max}). (a) In the absence of nitrate, red shift of λ_{max} was observed, indicating the restoration of π-conjugated structures; (b) in the presence of nitrate, blue shift of λ_{max} was observed, indicating the damage of the local π-conjugated structures of GO sheets.

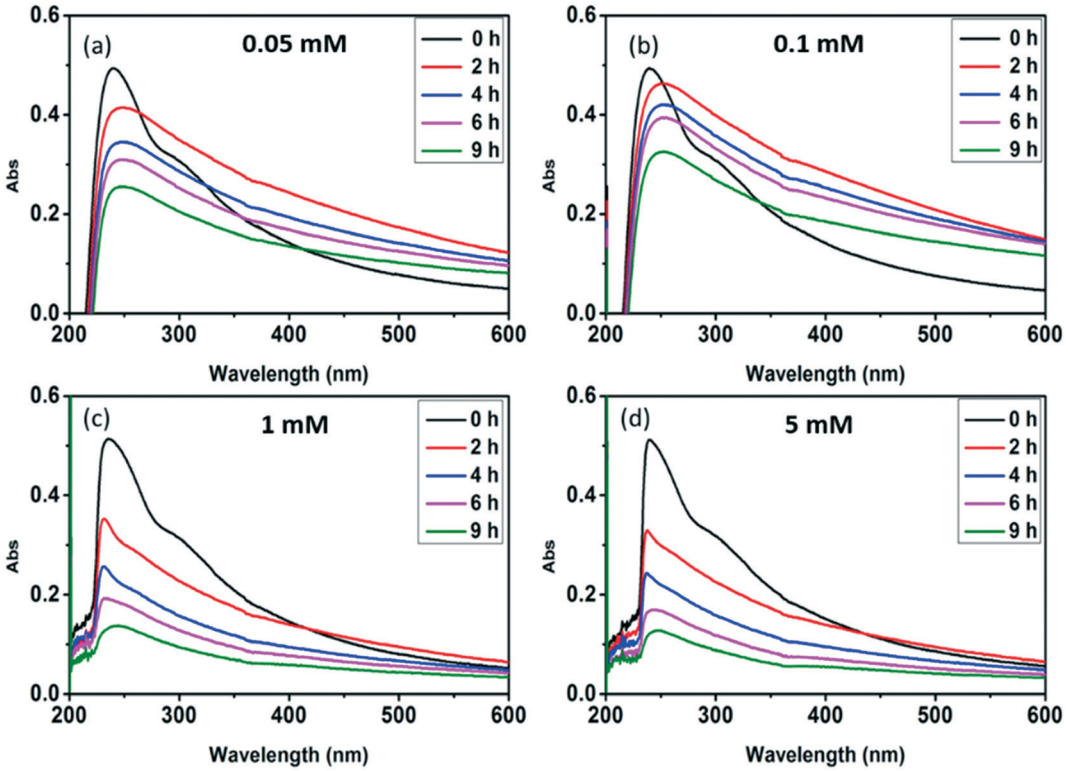

Fig. 3 UV-vis spectra of 10 mg L^{-1} GO suspensions before and after UV irradiation in the presence of nitrate at different concentrations (a: 0.05 mM; b: 0.1 mM; c: 1 mM; and d: 5 mM), showing the concentration-dependent effects of nitrate on the structural changes of GO nanosheets. Red shift of λ_{max} of GO suspension was observed at nitrate concentrations of 0.05 and 0.1 mM, whereas blue shift of λ_{max} was observed at nitrate concentrations of 1 and 5 mM.

spectra of both GO-UV and GO-UV-nitrate (ESI† Fig. S9), indicating fragmentation of GO nanosheets; this is consistent with the findings of Hou *et al.*[14] However, for GO-UV-nitrate, the photolysis products in the higher mass-to-charge ratio (*m*/*z*) range (*i.e.*, 700–1000) almost disappeared, whereas these products remained for GO-UV. This further corroborated the more significant fragmentation of GO nanostructure for GO-UV-nitrate than that for GO-UV. This observation may have important implications as small toxic organic molecules (*e.g.*, oxygenated polycyclic aromatic hydrocarbon species) might be formed from this process.[14,15] Consistently, a significant decrease of TOC concentration with irradiation time was observed for the experiment involving nitrate (ESI† Fig. S10), indicating that extensive degradation of GO occurred.

Changes of GO surface O-functionality. XPS analysis showed that after UV irradiation, the carbon-to-oxygen atom ratio (C/O) of both GO-UV and GO-UV-nitrate increased substantially compared to that of GO-dark, indicating that GO was reduced upon UV irradiation. Moreover, the carbon species distributions changed significantly, in that the intensity of C–C/C=C increased and intensity of C–O decreased for both GO-UV and GO-UV-nitrate (Table 1 and ESI† Fig. S11), consistent with previous studies on UV induced GO transformation.[19,20] Notably, GO-UV-nitrate contained markedly greater amount of C–O (20.59%) than GO-UV (14.18%), but significantly smaller amount of O–C=O (4.96%) than GO-UV (10.68%), indicating that the presence of nitrate resulted in surface oxide formation of GO.

3.2 Identification of ROS responsible for nitrate-induced indirect photolysis of GO

Photolysis of nitrate is known to produce different ROS, including $^{\bullet}NO$ or $^{\bullet}NO_2$, $O_2^{\bullet-}$ and $^{\bullet}OH$,[29,32,35,36] which may contribute to the indirect photolysis of GO. Nitrogen oxide radicals ($^{\bullet}NO$ and $^{\bullet}NO_2$) are weaker oxidants compared to $^{\bullet}OH$, and can be rapidly recombined to form nitrate.[35,36] Accordingly, these two ROS likely were not important species

Table 1 Surface chemical properties of graphene oxide (GO) samples obtained from X-ray photoelectron spectroscopy

Sample ID	C species (wt%)				C/O ratio
	C–C/C=C	C–O	C=O	O–C=O	
GO-dark[a]	46.67	40.59	10.31	2.42	2.40
GO-UV[b]	72.89	14.18	2.23	10.68	4.28
GO-UV-nitrate[c]	70.85	20.59	3.60	4.96	3.93

[a] "GO-dark" represents the GO sample without UV irradiation (kept in dark condition). [b] "GO-UV" represents the GO product after 9 h of UV irradiation in DI water. [c] "GO-UV-nitrate" represents the GO product after 9 h of UV irradiation in the presence of nitrate (1 mM).

responsible for the significant indirect photolysis of GO. Since deoxygenation of the reaction matrix did not inhibit the significant disintegration of GO sheets (Fig. 4a and ESI† Fig. S12), $O_2^{\cdot-}$ likely was not an important ROS responsible to the observed effects of nitrate on GO transformation. Interestingly, the addition of 1% isopropylamine, a scavenger of $^{\cdot}OH$,[41] greatly inhibited the disintegration of GO nanosheets (Fig. 4b), as the color of the suspension turned blackish instead of becoming clear, similar to the appearance of the suspension of GO-UV (Fig. 1b). This result indicated that the nitrate-induced indirect photolysis of GO was mainly caused by the photo-generated $^{\cdot}OH$.

To further verify that $^{\cdot}OH$ was the predominant ROS responsible for the nitrate-induced indirect photolysis of GO, we conducted supplemental experiments using N_2O-saturated water under steady-state γ-radiation, a condition known to generate only $^{\cdot}OH$.[26,42] The color of the GO suspension became gradually transparent when receiving increasing doses of γ-radiation (400, 800, 1600 and 3000 Gy, Fig. 4c) (*i.e.*, the concentration of $^{\cdot}OH$ increased with the increasing dose of γ-radiation). Consistently, the characteristic peak of GO centered at 230 nm of the UV-vis spectrum gradually disappeared during γ-radiolysis (ESI† Fig. S13), indicating molecular alteration due to the reaction of GO with $^{\cdot}OH$.[43] These trends are consistent with that observed for GO-UV-nitrate (Fig. 1c), confirming that nitrate-induced indirect photolysis of GO occurred primarily through a $^{\cdot}OH$-induced pathway.

Radical trapping experiment using pCBA as the $^{\cdot}OH$ probe showed that the steady-state concentrations of $^{\cdot}OH$ ($[^{\cdot}OH]_{ss}$) in the GO suspension during UV-irradiation with nitrate increased with increasing nitrate concentration (from 1.6×10^{-14} M for 0.05 mM nitrate to 1.35×10^{-13} M for 5 mM nitrate) (Fig. 5), indicating that the generation of $^{\cdot}OH$ was dependent on nitrate concentration and was consistent with the concentration-dependent effects of nitrate on GO transformation (Fig. 3). Note that the amount of $^{\cdot}OH$ generated in the system containing only GO (*i.e.*, in the absence of nitrate) can be neglected when compared with the systems containing both GO and nitrate (Fig. 5), which was likely related to the inhibition of $^{\cdot}OH$ through UV absorption and scavenging of $^{\cdot}OH$ by GO. This is consistent with previous research by Zhao and Jafvert[41] showing that upon solar light irradiation of single layered GO dispersed in water, only a

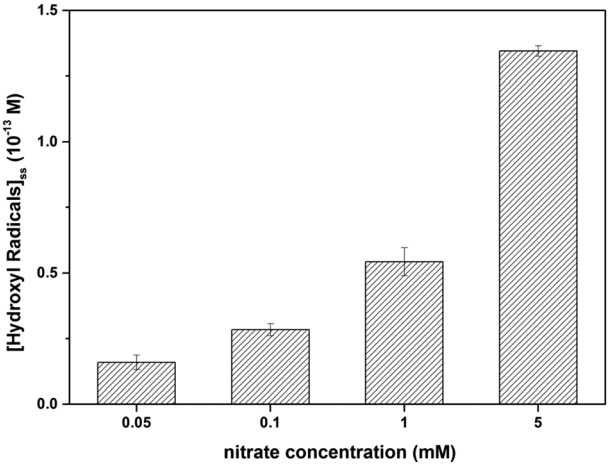

Fig. 5 Production of $^{\cdot}OH$ under UV irradiation of 10 mg L^{-1} GO suspension, as affected by the concentration of nitrate (0.05, 0.1, 1 and 5 mM), showing that the concentration of $^{\cdot}OH$ was dependent upon the nitrate concentration (the $[^{\cdot}OH]_{ss}$ generated in the system containing only GO was minimal and calibrated to zero).

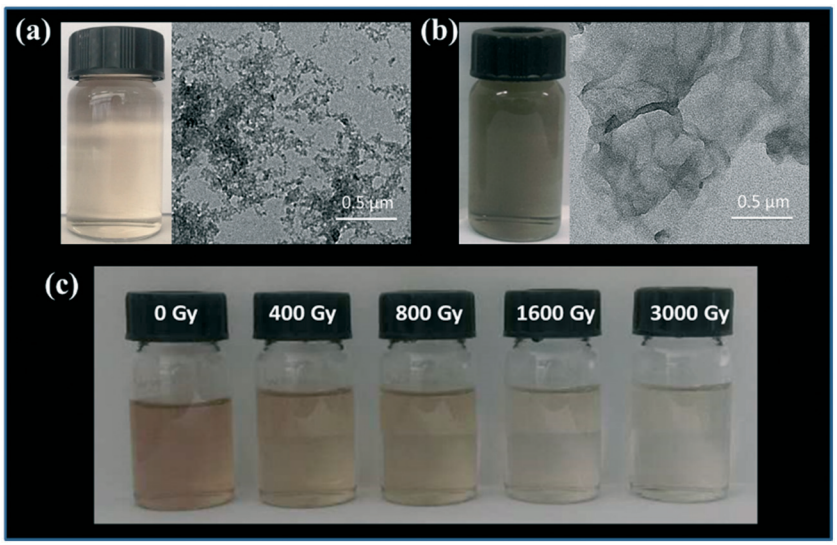

Fig. 4 Transformation of GO in aqueous suspension (10 mg L^{-1}) under different conditions, showing that $^{\cdot}OH$ was responsible for nitrate-induced indirect photolysis of GO. (a) Anaerobic experiments: 10 mg L^{-1} GO in 1 mM nitrate solution purged with 99.99% N_2 prior to UV irradiation; significant fragmentation of GO nanosheets without dissolved O_2 was observed; (b) ROS inhibition experiments: 10 mg L^{-1} GO in 1 mM nitrate with the presence of 1% isopropylamine (as a scavenger of $^{\cdot}OH$), and no fragmentation of GO sheets was observed; (c) γ-radiolysis experiments: 10 mg L^{-1} GO irradiated with steady-state γ-radiation under N_2O saturated conditions; the color of GO suspension gradually turned to nearly transparent after receiving increasing doses of γ-radiation, which verified the contribution of $^{\cdot}OH$.

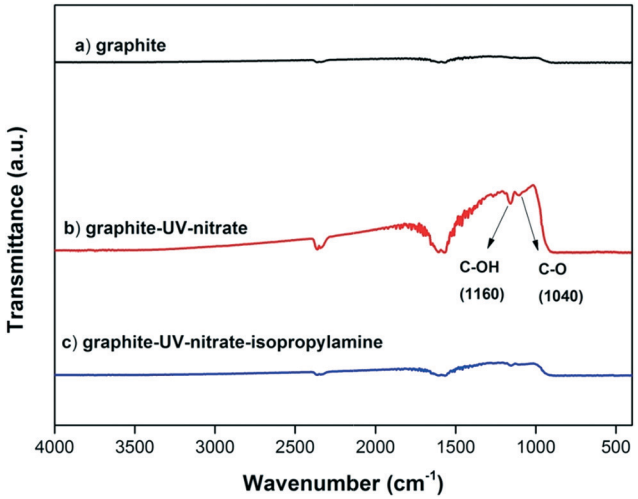

Fig. 6 FTIR spectra of graphite (40 mg L^{-1}) before and after UV irradiation in the presence of nitrate, showing that photo-generated ˙OH forms O-functional groups on graphite surface. (a) Graphite (without irradiation); (b) graphite-UV-nitrate (irradiation of a graphite suspension in the presence of 4 mM nitrate); (c) graphite-UV-nitrate-isopropylamine (irradiation of a graphite suspension in the presence of 4 mM nitrate and 1% (v/v) isopropylamine). The absorption bands around 1160 cm^{-1} and 1040 cm^{-1} are ascribed to the vibrations of C–OH and C–O, which were observed only for graphite-UV-nitrate, indicating that oxidation reaction(s) occurred between ˙OH and the aromatic structure of graphite.

negligible amount of ˙OH was detected, mainly because the scavenging of ˙OH by GO was likely rapid and significant.

3.3 Proposed reaction pathways for nitrate-induced indirect photolysis of GO

GO contains both oxidized domains and aromatic domains.[44] It has been proposed that the indirect photolysis of GO occurs mainly through the oxidation reactions between ˙OH and the O-functional groups of GO, and the reaction rate depends strongly on the oxidization extent of GO.[15,23,36] However, it has also been reported that the aromatic domains of GO were the primary site to scavenge ROS,[27] suggesting that the oxidation reaction likely occurred at the aromatic domains of GO.[27] Consistently, we hypothesize that the aromatic domains are also susceptible to the oxidation by ˙OH.

To determine whether the aromatic domains of GO can directly react with ˙OH during the indirect photolysis of GO, an ROS inhibition experiment using isopropylamine as ˙OH scavenger was conducted using the functionality-free, pure graphite (99.99% C) as a model material. As expected, FTIR analysis showed that in the presence of nitrate, the absorption bands around 1160 cm^{-1} and 1040 cm^{-1} (which are ascribed to C–OH and C–O) appeared on graphite upon UV irradiation,[45] indicating that the O-functionality-free aromatic structures of graphite were reactive toward ˙OH; however, when isopropylamine was added, no observable amounts of O-functional groups were formed on graphite surfaces (Fig. 6). These results support the hypothesis that ˙OH oxidized the aromatic domains of GO.

On the basis of these observations and the literature,[46] we postulate that ˙OH reacted with the aromatic rings of GO surface *via* electrophilic addition reactions, forming hydroxylated GO, which underwent further oxidation. The direct attack of ˙OH on the π-conjugated structures of GO can cause ring cleavage of the aromatic moieties, in a similar way to the ring cleavage process that occurred during ozonation of dissolved organic matter.[47] The oxidation of the aromatic rings of GO *via* electrophilic addition reaction is consistent with the difference in carbon species distribution manifested by comparing the XPS results between GO-UV and GO-UV-nitrate (Table 1 and ESI† Fig. S11). For instance, the C–O content of GO-UV-nitrate (20.59%) was significantly higher than that of GO-UV (14.18%), which was probably due to the newly formed hydroxyl groups on GO. Interestingly, the O–C=O

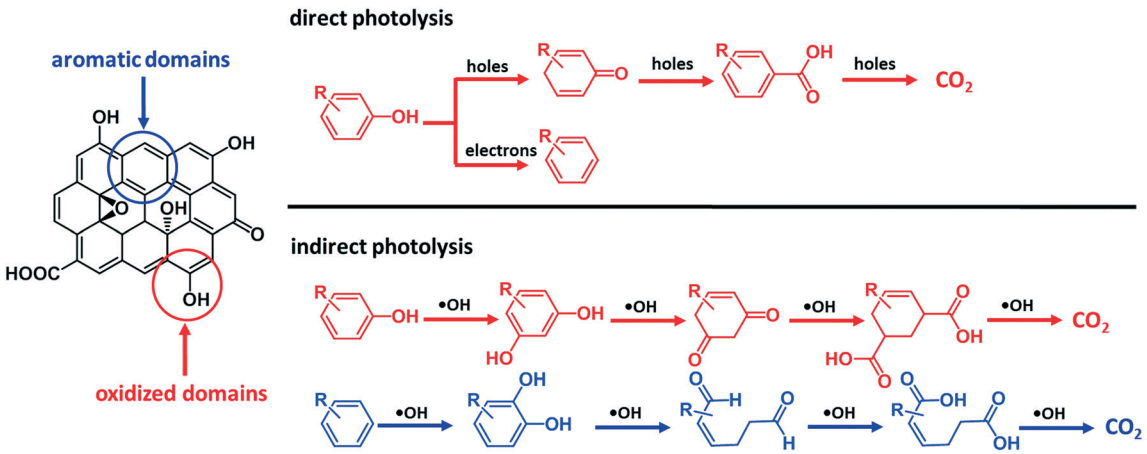

Fig. 7 Proposed direct and indirect pathways for the photolysis of GO under UV irradiation. Direct photolysis occurs mainly through the reactions between photo induced electron–hole pairs and the oxidized domains of GO (shown with red circle), in that, reduction by photo induced electrons results in the restoration of the aromatic domains of GO, and the oxidation of O-functional groups by holes converts O-functional groups to higher oxidation state (quinones and carboxylic acids). Indirect photolysis of GO occurs primarily through the oxidation of both the oxidized domains and aromatic domains (shown with blue circle) of GO by nitrate induced ˙OH.

content of GO-UV-nitrate (4.96%) was significantly lower than that of GO-UV (10.68%), which was likely due to the decarboxylation of the carboxylic acids of GO. Fig. 7 illustrates these predominant reaction pathways of indirect photolysis by nitrate-induced $^{\bullet}$OH *versus* direct photolysis by photo induced electron–hole pairs.

4 Conclusions

Direct and indirect photolysis of GO lead to drastically different transformation products, which may exhibit dissimilar properties. Our study suggests that the significant effects of nitrate on GO photolysis were due to the indirect photolysis mediated by nitrate-induced $^{\bullet}$OH. Specifically, when reaching a concentration threshold of nitrate (*e.g.*, 1 mM under the experimental conditions of the present study), the dominant reaction pathway of GO photolysis changed from direct photolysis to indirect photolysis. The concentration of nitrate is critical for determining the relative contributions of the direct *vs.* indirect photolysis pathways.

The indirect photolysis pathway resulted in damage of the local π-conjugated structures, whereas direct photolysis resulted in restoration of π-conjugated structures. Notably, the indirect photolysis of GO mediated by $^{\bullet}$OH was not only driven by the oxidation reactions between $^{\bullet}$OH and oxidized domains, but also by the electrophilic addition reactions of $^{\bullet}$OH to the aromatic domains, causing substantial disintegration of GO nanostructures. The findings of this study underline the importance of indirect photolysis of GO in the presence of ROS precursors, and may have important implications for GO integrity and durability when used in water and wastewater treatment devices.

Conflicts of interest

There are no conflicts to declare.

Acknowledgements

This project was supported by the National Natural Science Foundation of China (Grants 41603099 and 21425729), Tianjin Municipal Science and Technology Commission (Grants 16JCYBJC22400, 17JCYBJC23100 and 17JCYBJC23200), the Ministry of Science and Technology of China (Grant 2014CB932001), the Fundamental Research Funds for the Central Universities and the 111 Program of Ministry of Education of China (T2017002). Partial funding was provided by the NSF ERC on Nanotechnology-Enabled Water Treatment (EEC-1449500).

References

1 X. Huang, Z. Yin, S. Wu, X. Qi, Q. He, Q. Zhang, Q. Yan, F. Boey and H. Zhang, Graphene-Based Materials: Synthesis, Characterization, Properties, and Applications, *Small*, 2011, **7**, 1876–1902.

2 Y. H. Ng, S. Ikeda, M. Matsumura and R. Amal, A perspective on fabricating carbon-based nanomaterials by photocatalysis and their applications, *Energy Environ. Sci.*, 2012, **5**, 9307–9318.

3 H. Chang and H. Wu, Graphene-based nanocomposites: preparation, functionalization, and energy and environmental applications, *Energy Environ. Sci.*, 2013, **6**, 3483–3507.

4 K. C. Kemp, H. Seema, M. Saleh, N. H. Le, K. Mahesh, V. Chandra and K. S. Kim, Environmental applications using graphene composites: water remediation and gas adsorption, *Nanoscale*, 2013, **5**, 3149–3171.

5 F. Perreault, A. Fonseca de Faria and M. Elimelech, Environmental applications of graphene-based nanomaterials, *Chem. Soc. Rev.*, 2015, **44**, 5861–5896.

6 S. C. Smith and D. F. Rodrigues, Carbon-based nanomaterials for removal of chemical and biological contaminants from water: A review of mechanisms and applications, *Carbon*, 2015, **91**, 122–143.

7 X. Zhu, K. Yang and B. Chen, Membranes prepared from graphene-based nanomaterials for sustainable applications: a review, *Environ. Sci.: Nano*, 2017, **4**, 2267–2285.

8 Z. Cai, A. D. Dwivedi, W.-N. Lee, X. Zhao, W. Liu, M. Sillanpaa, D. Zhao, C.-H. Huang and J. Fu, Application of nanotechnologies for removing pharmaceutically active compounds from water: development and future trends, *Environ. Sci.: Nano*, 2018, **5**, 27–47.

9 P. Westerhoff, P. Alvarez, Q. Li, J. Gardea-Torresdey and J. Zimmerman, Overcoming implementation barriers for nanotechnology in drinking water treatment, *Environ. Sci.: Nano*, 2016, **3**, 1241–1253.

10 Y. Shen, Q. Fang and B. Chen, Environmental Applications of Three-Dimensional Graphene-Based Macrostructures: Adsorption, Transformation, and Detection, *Environ. Sci. Technol.*, 2015, **49**, 67–84.

11 Y. Li, N. Yang, T. Du, X. Wang and W. Chen, Transformation of graphene oxide by chlorination and chloramination: Implications for environmental transport and fate, *Water Res.*, 2016, **103**, 416–423.

12 Y. Li, N. Yang, T. Du, T. Xia, C. Zhang and W. Chen, Chloramination of graphene oxide significantly affects its transport properties in saturated porous media, *NanoImpact*, 2016, **3–4**, 90–95.

13 X. Ren, J. Li, C. Chen, Y. Gao, D. Chen, M. Su, A. Alsaedi and T. Hayat, Graphene analogues in aquatic environments and porous media: dispersion, aggregation, deposition and transformation, *Environ. Sci.: Nano*, 2018, **5**, 1298–1340.

14 W.-C. Hou, I. Chowdhury, D. G. Goodwin, W. M. Henderson, D. H. Fairbrother, D. Bouchard and R. G. Zepp, Photochemical Transformation of Graphene Oxide in Sunlight, *Environ. Sci. Technol.*, 2015, **49**, 3435–3443.

15 H. Bai, W. Jiang, G. P. Kotchey, W. A. Saidi, B. J. Bythell, J. M. Jarvis, A. G. Marshall, R. A. S. Robinson and A. Star, Insight into the Mechanism of Graphene Oxide Degradation via the Photo-Fenton Reaction, *J. Phys. Chem. C*, 2014, **118**, 10519–10529.

16 W. A. M. Hijnen, E. F. Beerendonk and G. J. Medema, Inactivation credit of UV radiation for viruses, bacteria and

protozoan (oo)cysts in water: A review, *Water Res.*, 2006, **40**, 3–22.

17 H. Liu, S. Ryu, Z. Chen, M. L. Steigerwald, C. Nuckolls and L. E. Brus, Photochemical Reactivity of Graphene, *J. Am. Chem. Soc.*, 2009, **131**, 17099–17101.

18 O. Akhavan, M. Abdolahad, A. Esfandiar and M. Mohatashamifar, Photodegradation of Graphene Oxide Sheets by TiO_2 Nanoparticles after a Photocatalytic Reduction, *J. Phys. Chem. C*, 2010, **114**, 12955–12959.

19 Y. Matsumoto, M. Koinuma, S. Y. Kim, Y. Watanabe, T. Taniguchi, K. Hatakeyama, H. Tateishi and S. Ida, Simple Photoreduction of Graphene Oxide Nanosheet under Mild Conditions, *ACS Appl. Mater. Interfaces*, 2010, **2**, 3461–3466.

20 Y. Matsumoto, M. Koinuma, S. Ida, S. Hayami, T. Taniguchi, K. Hatakeyama, H. Tateishi, Y. Watanabe and S. Amano, Photoreaction of Graphene Oxide Nanosheets in Water, *J. Phys. Chem. C*, 2011, **115**, 19280–19286.

21 L. Guardia, S. Villar-Rodil, J. I. Paredes, R. Rozada, A. Martínez-Alonso and J. M. D. Tascón, UV light exposure of aqueous graphene oxide suspensions to promote their direct reduction, formation of graphene–metal nanoparticle hybrids and dye degradation, *Carbon*, 2012, **50**, 1014–1024.

22 M. Koinuma, C. Ogata, Y. Kamei, K. Hatakeyama, H. Tateishi, Y. Watanabe, T. Taniguchi, K. Gezuhara, S. Hayami, A. Funatsu, M. Sakata, Y. Kuwahara, S. Kurihara and Y. Matsumoto, Photochemical Engineering of Graphene Oxide Nanosheets, *J. Phys. Chem. C*, 2012, **116**, 19822–19827.

23 X. Zhou, Y. Zhang, C. Wang, X. Wu, Y. Yang, B. Zheng, H. Wu, S. Guo and J. Zhang, Photo-Fenton Reaction of Graphene Oxide: A New Strategy to Prepare Graphene Quantum Dots for DNA Cleavage, *ACS Nano*, 2012, **6**, 6592–6599.

24 T. Ji, Y. Hua, M. Sun and N. Ma, The mechanism of the reaction of graphite oxide to reduced graphene oxide under ultraviolet irradiation, *Carbon*, 2013, **54**, 412–418.

25 Y.-L. Zhang, L. Guo, H. Xia, Q.-D. Chen, J. Feng and H.-B. Sun, Photoreduction of Graphene Oxides: Methods, Properties, and Applications, *Adv. Opt. Mater.*, 2014, **2**, 10–28.

26 C. Yu, B. Zhang, F. Yan, J. Zhao, J. Li, L. Li and J. Li, Engineering nano-porous graphene oxide by hydroxyl radicals, *Carbon*, 2016, **105**, 291–296.

27 Y. Qiu, Z. Wang, A. C. E. Owens, I. Kulaots, Y. Chen, A. B. Kane and R. H. Hurt, Antioxidant chemistry of graphene-based materials and its role in oxidation protection technology, *Nanoscale*, 2014, **6**, 11744–11755.

28 A. Ianoul, T. Coleman and S. A. Asher, UV Resonance Raman Spectroscopic Detection of Nitrate and Nitrite in Wastewater Treatment Processes, *Anal. Chem.*, 2002, **74**, 1458–1461.

29 C. M. Sharpless and K. G. Linden, UV Photolysis of Nitrate: Effects of Natural Organic Matter and Dissolved Inorganic Carbon and Implications for UV Water Disinfection, *Environ. Sci. Technol.*, 2001, **35**, 2949–2955.

30 M. Zhan, X. Yang, Q. Xian and L. Kong, Photosensitized degradation of bisphenol A involving reactive oxygen species in the presence of humic substances, *Chemosphere*, 2006, **63**, 378–386.

31 D. Zhang, S. Yan and W. Song, Photochemically Induced Formation of Reactive Oxygen Species (ROS) from Effluent Organic Matter, *Environ. Sci. Technol.*, 2014, **48**, 12645–12653.

32 P. L. Brezonik and J. Fulkerson-Brekken, Nitrate-Induced Photolysis in Natural Waters: Controls on Concentrations of Hydroxyl Radical Photo-Intermediates by Natural Scavenging Agents, *Environ. Sci. Technol.*, 1998, **32**, 3004–3010.

33 O. S. Keen, N. G. Love and K. G. Linden, The role of effluent nitrate in trace organic chemical oxidation during UV disinfection, *Water Res.*, 2012, **46**, 5224–5234.

34 R. C. Sandford, A. Exenberger and P. J. Worsfold, Nitrogen Cycling in Natural Waters using In Situ, Reagentless UV Spectrophotometry with Simultaneous Determination of Nitrate and Nitrite, *Environ. Sci. Technol.*, 2007, **41**, 8420–8425.

35 J. Mack and J. R. Bolton, Photochemistry of nitrite and nitrate in aqueous solution: a review, *J. Photochem. Photobiol., A*, 1999, **128**, 1–13.

36 D.-H. Kim, J. Lee, J. Ryu, K. Kim and W. Choi, Arsenite Oxidation Initiated by the UV Photolysis of Nitrite and Nitrate, *Environ. Sci. Technol.*, 2014, **48**, 4030–4037.

37 F. Wang, F. Wang, G. Gao and W. Chen, Transformation of graphene oxide by ferrous iron: Environmental implications, *Environ. Toxicol. Chem.*, 2015, **34**, 1975–1982.

38 J. Lee, M. Cho, J. D. Fortner, J. B. Hughes and J.-H. Kim, Transformation of Aggregated C_{60} in the Aqueous Phase by UV Irradiation, *Environ. Sci. Technol.*, 2009, **43**, 4878–4883.

39 J. L. Bitter, J. Yang, S. Beigzadeh Milani, C. T. Jafvert and D. H. Fairbrother, Transformations of oxidized multiwalled carbon nanotubes exposed to UVC (254 nm) irradiation, *Environ. Sci.: Nano*, 2014, **1**, 324–337.

40 I. Chowdhury, W.-C. Hou, D. Goodwin, M. Henderson, R. G. Zepp and D. Bouchard, Sunlight affects aggregation and deposition of graphene oxide in the aquatic environment, *Water Res.*, 2015, **78**, 37–46.

41 Y. Zhao and C. T. Jafvert, Environmental photochemistry of single layered graphene oxide in water, *Environ. Sci.: Nano*, 2015, **2**, 136–142.

42 A. Ansón-Casaos, J. A. Puértolas, F. J. Pascual, J. Hernández-Ferrer, P. Castell, A. M. Benito, W. K. Maser and M. T. Martínez, The effect of gamma-irradiation on few-layered graphene materials, *Appl. Surf. Sci.*, 2014, **301**, 264–272.

43 J. Lee, W. Song, S. S. Jang, J. D. Fortner, P. J. J. Alvarez, W. J. Cooper and J.-H. Kim, Stability of Water-Stable C_{60} Clusters to OH Radical Oxidation and Hydrated Electron Reduction, *Environ. Sci. Technol.*, 2010, **44**, 3786–3792.

44 S. Pei and H.-M. Cheng, The reduction of graphene oxide, *Carbon*, 2012, **50**, 3210–3228.

45 S.-H. Hwang, D. Kang, R. S. Ruoff, H. S. Shin and Y.-B. Park, Poly(vinyl alcohol) Reinforced and Toughened with

Poly(dopamine)-Treated Graphene Oxide, and Its Use for Humidity Sensing, *ACS Nano*, 2014, **8**, 6739–6747.

46 S. Gligorovski, R. Strekowski, S. Barbati and D. Vione, Environmental Implications of Hydroxyl Radicals (˙OH), *Chem. Rev.*, 2015, **115**, 13051–13092.

47 J. Wenk, M. Aeschbacher, E. Salhi, S. Canonica, U. von Gunten and M. Sander, Chemical Oxidation of Dissolved Organic Matter by Chlorine Dioxide, Chlorine, And Ozone: Effects on Its Optical and Antioxidant Properties, *Environ. Sci. Technol.*, 2013, **47**, 11147–11156.